

Structure of $(\sqrt{3} \times \sqrt{3})R30^\circ$ Ag on Si(111)

E. L. Bullock,* G. S. Herman, M. Yamada,† D. J. Friedman, and C. S. Fadley

Department of Chemistry, University of Hawaii, Honolulu, Hawaii 96822

(Received 1 November 1989)

The structure of $(\sqrt{3} \times \sqrt{3})R30^\circ$ Ag on Si(111) has been studied by polar and azimuthal x-ray photoelectron diffraction. We conclude from this data that the Ag cannot be more than 0.5 Å below the surface, and furthermore from an *R*-factor analysis of the azimuthal results that the structure consists of two closely related types of Ag honeycomb domains that grow on the second Si layer, with the top Si layer missing.

The $(\sqrt{3} \times \sqrt{3})R30^\circ$ structure of Ag on Si(111) has been studied by almost every technique in surface science.¹⁻¹⁰ This list includes low-energy electron diffraction (LEED),^{1,2} reflection high-energy electron diffraction (RHEED),³ scanning-tunneling microscopy (STM),⁴ impact-collision ion-scattering spectroscopy (ICISS),⁵ surface extended x-ray absorption fine structure (SEX-AFS),⁶ surface x-ray diffraction (XRD),⁷ medium-energy ion scattering (MEIS),⁸ and x-ray photoelectron diffraction (XPD).⁹ In spite of this effort, there is still no consensus on the atomic geometry of this structure, with several new proposals being made very recently.^{2,3(b),5(b),5(c),7,8} Two separate STM studies have reached different conclusions concerning this structure, with one proposing that the regular honeycomb pattern seen in the images is caused by surface Si atoms^{4(a)} and the other that it is due to Ag atoms.^{4(b)} A recent Letter² has also proposed that the Ag has no long-range order, and may be either buried within the first few layers of the surface or present as islands or clusters on the surface. Debate also continues over whether the Ag coverage is $\frac{2}{3}$ or 1 ML and whether 1 ML is essential for producing the observed semiconducting character of this surface.^{4(a),10(b)}

In order to resolve some of these questions, we have studied this system using x-ray photoelectron diffraction in a more complete way than in a prior investigation by Kono, Higashiyama, and Sagawa.⁹ We have used both polar and azimuthal scans of the Ag $3d_{5/2}$ intensity in determining the structure, whereas the prior study only reported azimuthal data. We have also used azimuthal data scanned over a full 360° range and threefold-averaged them into 120° for analysis; such data should be less influenced by slight crystal misalignments, which are easily seen as asymmetries from one 120° interval to another. The prior study involved only a minimum 70° scan range. In analyzing our data with single-scattering cluster diffraction calculations,¹¹ our final results incorporate the correct spherical-wave nature of the final-state photoelectron waves, as well as the various angular momenta and interferences involved because of the *d*-to-*p* + *f* dipole transition.¹² Prior analyses of XPD data have usually assumed an *s*-to-*p* transition for simplicity, and have often been based upon plane-wave scattering.^{9,11} Finally, in comparing experimental and theoretical azimuthal curves for different structures, we have used *R* factors¹³ as

a quantitative measure of the goodness of fit, whereas prior work has been based upon visual comparisons. The same nonstructural parameters of inner potential (12 eV), electron attenuation length (13 Å), Debye-Waller factors, and muffin-tin scattering phase shifts have been used for all structures tested, although our structural conclusions were not found to be sensitive to these choices.

The measurements were performed on a combined XPD-LEED system (HP 5950A) that is described elsewhere.^{11(a)} The sample was a mirror-polished Si wafer (B doped, 0.25 Ω cm) oriented to within $\pm 0.4^\circ$ of (111). This was chemically cleaned in a multistep process.¹⁴ Such surfaces exhibited excellent (7×7) LEED patterns after ion bombardment and annealing in vacuum to about 1150°C. The $(\sqrt{3} \times \sqrt{3})R30^\circ$ Ag structure was formed by depositing about 1.3 ML of Ag on a surface heated to 550°C, a procedure very close to that of other studies.^{4,9} Very sharp $(\sqrt{3} \times \sqrt{3})$ LEED patterns were seen, and the surface was very stable against contamination, remaining clean as judged by x-ray photoelectron spectroscopy (XPS) for as long as four weeks in our vacuum of $< 2 \times 10^{-10}$ torr. From XPS intensity ratios for Ag $3d_{5/2}$ /Si $2p$, we determine a Ag coverage of 0.82 ± 0.16 ML; this is in very good agreement with a recent value of 0.85 ± 0.05 from medium-energy ion scattering.⁸ Our number is thus consistent with either a $\frac{2}{3}$ - or 1-ML coverage.

We consider first polar-scan data, as shown in Fig. 1. In a series of measurements, a thick overlayer of Ag of about 6 ML in average thickness was deposited at room temperature, and then the surface was heated in steps up to 550°C, at which point the only remaining Ag is in the $(\sqrt{3} \times \sqrt{3})$ structure. Polar scans are shown in several high-symmetry azimuths, with $\phi = 0^\circ$ being defined as the [11, -2] direction. The polar angle is defined with respect to the surface; instrumental effects cause a decrease of all intensities as θ goes to zero.^{11(a)} For a thick Ag overlayer in Fig. 1(c), we find the pronounced peaks characteristic of the expected epitaxial growth of Ag with (111) orientation.¹⁵ They are due to near-neighbor forward scattering effects and higher-order diffraction features which are expected to occur for such high-energy photoelectrons (kinetic energy ≈ 1126 eV) as they leave this epitaxial fcc lattice.^{11(b),11(c)} As the temperature is raised to 450°C in Fig. 1(b) so as to yield an average overlayer thickness as judged by XPS of 2 ML, these peaks begin to disappear;

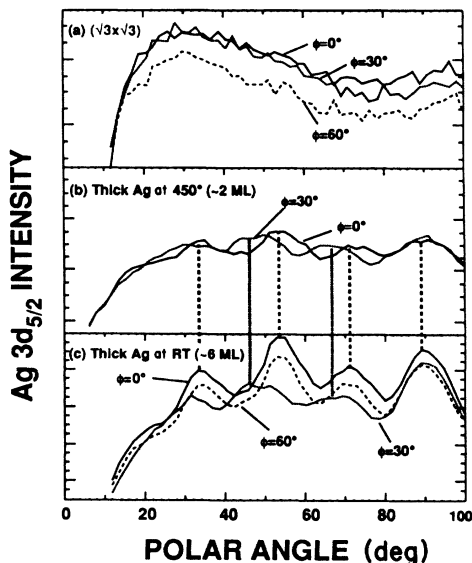


FIG. 1. Polar scans of Ag $3d_{5/2}$ intensity from (a) the $(\sqrt{3}\times\sqrt{3})R30^\circ$ Ag structure formed after an anneal to 550°C , (b) a Ag overlayer of approximately 2-ML average thickness at 450°C , and (c) a thick Ag overlayer of approximately 6-ML thickness at ambient temperature.

however, comparing the weak features which remain with those in Fig. 1(c) indicates the continuing presence of Ag with (111) orientation, perhaps in two-dimensional (2D) islands or 3D microclusters. After annealing at 550°C and returning to room temperature in Fig. 1(a) so as to desorb all but $(\sqrt{3}\times\sqrt{3})$ Ag, we see curves for all three high-symmetry azimuths that are very smooth and without any of the fine structure expected from near-neighbor forward scattering. Prior XPD and Auger diffraction studies of forward scattering and epitaxial-overlayer growth¹¹ permit us to conclude from these results that the $(\sqrt{3}\times\sqrt{3})$ Ag atoms are neither buried under other Ag atoms in microclusters of ≥ 2 ML thickness nor present to any degree as species deeply buried under the Si surface.

As a more quantitative indicator of the maximum depth at which Ag can be below the Si surface, we note that forward-scattering peaks do appear to be present in our azimuthal data for low takeoff angles from 4° up to about $8\text{--}10^\circ$ (quartet of peaks in the bottom experimental curves of Fig. 2). The fact that these peaks decay away and become more complex by about 10° , and that the overall diffraction anisotropy $\Delta I/I_{\text{max}}$ dies away to only a few percent by $\theta=20^\circ$, both argue that the relevant Ag nearest-neighbor forward-scattering angle is not larger than about 10° relative to the surface. For typical expected bond distances of 2.7 \AA for Ag-Si (Ref. 10) or 2.9 \AA for Ag-Ag, this yields a maximum depth below the surface of $z = -0.5 \text{ \AA}$. These combined polar and azimuthal results thus make any model with Ag buried more than 0.5 \AA below the Si surface very doubtful. Nonetheless, in testing different structures against our azimuthal data below, we have for completeness included every structure of which we are aware, regardless of its z value.

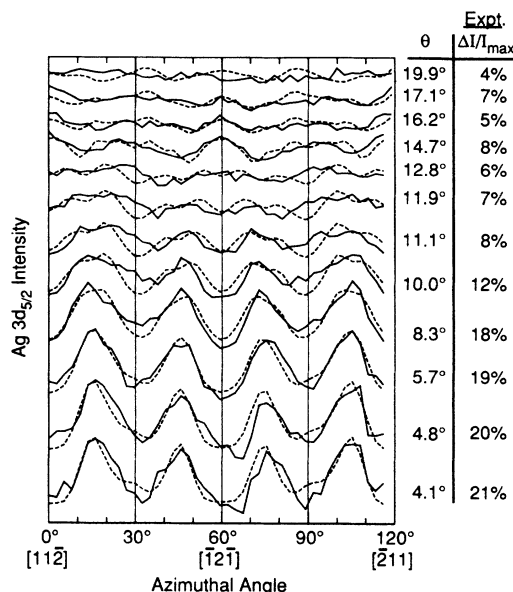


FIG. 2. Experimental and calculated azimuthal scans of Ag $3d_{5/2}$ intensity at various polar angles with respect to the surface from 4° to 20° . The calculated curves include correct d -to- p + f emission and are for the fully optimized two-domain model of Fig. 3(b) with 50% domain 1, 50% domain 2, $z_1 = -0.1 \text{ \AA}$, $z_2 = -0.3 \text{ \AA}$, and $s_1 = s_2 = 0.86 \text{ \AA}$. These curves yield an R factor of 0.138 [open-circle point in Fig. 3(a)].

The analysis of our azimuthal data consisted of calculating diffraction curves for different structures and different θ values and then comparing the two by means of R factors. The R factor we use is equivalent to the $R1$ of van Hove, Tong, and Elconin,¹³ but spot checks with others of the $R2\text{--}R5$ mentioned in that work yielded identical final structural conclusions. Figure 3(a) summarizes our searches over many structures, with each curve representing a variation of Ag height relative to the first Si layer, and families of curves involving the variation of a parameter s describing the compression of either Si trimers in missing-top-layer (MTL) honeycomb models [see Fig. 3(b)] or Ag trimers in that type of model. Points are shown for various proposed structures for which we have simply used the geometric parameters proposed in each paper.

The lowest R factor found in this single-scattering analysis is for a new two-domain MTL Ag honeycomb model with a z distance of about -0.20 \AA and an s of 0.86 \AA . The two types of domains are shown in Fig. 3(b). In one, the Ag atoms of the honeycomb do not have a fourth-layer Si atom directly under them, and in the other, they do. The first of these domains is very nearly the structure proposed previously using XPD by Kono *et al.*,⁹ who found $z = -0.15 \text{ \AA}$ and $s = 0.66 \text{ \AA}$; however, the R value of about 0.23 shown for this structure as XPD-1 is significantly above our final optimized value of 0.14. More importantly, this single domain is not able to correctly predict the quartet of strong peaks for low θ values, since only two strong features at $\phi \approx 44^\circ$ and 76° are seen due to scattering from the Si nearest neighbors in

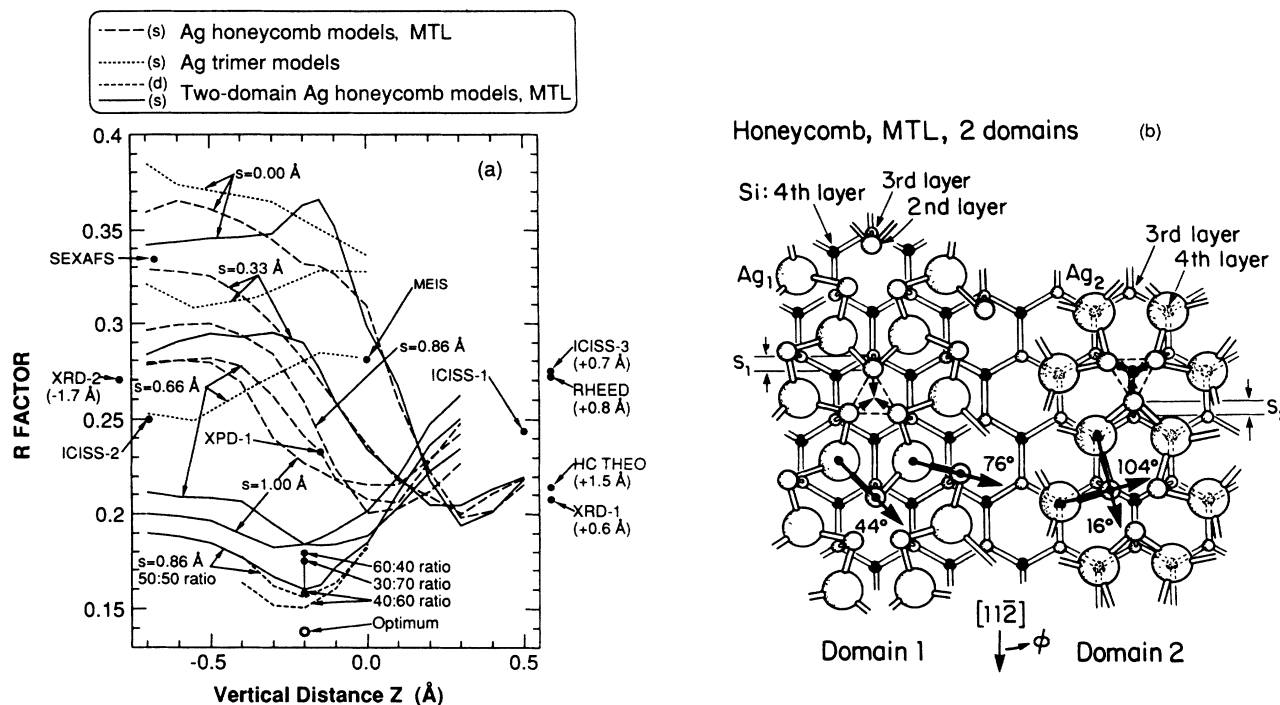


FIG. 3. (a) R factors for some of the structures tested against the experimental data of Fig. 2. Included are z scans for various choices of the contraction parameter s in the MTL Ag honeycomb (Ref. 9), the two-domain MTL Ag honeycomb proposed here, and the embedded trimer model suggested by STM [Ref. 4(a)], as well as single points for structures based upon different techniques as indicated: ICISS-1 [Ref. 5(a)], ICISS-2 [Ref. 5(b)], ICISS-3 [Ref. 5(c)], MEIS (Ref. 8), RHEED (Ref. 3), SEXAFS (Ref. 6), XPD-1 (Ref. 9), XRD-1 [Ref. 7(a)], and XRD-2 [Ref. 7(b)], and a theoretically determined structure for a full-double-layer Ag honeycomb (HC-theo) [Ref. 10(b)]. Structures falling outside of the z range are shown as points to left-hand side or right-hand side at the correct R values and with the z value indicated. The calculations for all curves except the bottom two were done with spherical-wave (SW) scattering and s -to- p emission; the bottom two dashed curves and the open-circle optimum point are SW with more accurate d -to- p + f emission. The open-circle point at lowest R is for the final fully optimized structure used in Fig. 2 with z_1 not equal to z_2 . (b) The two-domain missing-top-layer Ag honeycomb model proposed for the $(\sqrt{3}\times\sqrt{3})R30^\circ$ Ag structure. The two parameters characterizing it are the vertical heights z_1 and z_2 of Ag relative to the top Si layer [the second layer of the full Si(111) surface] and the contraction parameters s_1 and s_2 of the Si trimers in the top layer. In the bottom half of the figure are shown the two sets of nearest-neighbor-Si forward scattering peaks that produce the four-peak structure seen at low θ values in Fig. 2.

each compressed trimer (as verified by removing these atoms from the cluster). This is shown in the bottom half of Fig. 3(b), where the origin of the other two features at $\phi \approx 16^\circ$ and 104° arising in the second domain type are also indicated.

Although the distance of 2.8 Å between Ag in domain 2 and the fourth-layer Si atom below it in the absence of interlayer relaxation is not much larger than the 2.6 Å we find between this type of Ag and the topmost Si atoms, the fourth-layer atoms will retain their tetrahedral coordination to other Si atoms, and thus would not be expected to have a strong bonding interaction with Ag. Thus, the two types of domains may be very similar in their bonding and structure. It is therefore plausible for them both to form on a missing-top-layer surface, although perhaps not in identical quantities or with identical z and s values. We have thus further searched with R factor testing over various mixtures of the two domains and various structural parameters z_1 and z_2 , and s_1 and s_2 . Our final minimum R is 0.138 for an equal 50:50 mixture of the two domains with $z_1 = -0.1$ Å, $z_2 = -0.3$ Å, and $s_1 = s_2 = 0.86$ Å.

Thus, this single-scattering analysis predicts the mixing to be very nearly equal, and the two s and z values also to be about equal, as might be qualitatively expected. The final curves for this fully optimized model are compared directly to experiment in Fig. 2, where generally excellent agreement is seen. Only for the region of $\theta \approx 11^\circ$ – 13° over which the patterns change very rapidly with θ , and are thus less certain experimentally, are there a few features which disagree. Analogous comparisons of experiment and theory for any of the other structures previously proposed for this model are significantly poorer visually,¹⁶ and Fig. 3(a) of course also indicates that they have much higher R factors as well. Finally, we note that preliminary multiple scattering calculations by Kaduwela, Herman, Friedman, and Fadley¹⁷ show that the forward scattering peaks for both domains 1 and 2 shown in Fig. 3(b) are significantly reduced in intensity relative to adjacent features by defocussing effects, thereby improving the agreement between experimental and theoretical anisotropies, and also suggesting a stronger weighting of domain 1. Further multiple scattering analysis is in pro-

gress.

Although there are as yet no theoretical calculations for both of these MTL domains to test these models, first-principles total-energy estimates by Ho and Chan for domain 1 [Ref. 10(b)] yield a geometry with $z = 0.38 \text{ \AA}$ and $s = 0.75 \text{ \AA}$ that is in excellent agreement with our value for s and at least qualitatively in agreement with our z value in predicting a vertical distance relatively close to the Si layer.

Finally, we note that a recent Letter by Fan *et al.*² discussing LEED results for both $(\sqrt{3} \times \sqrt{3})R30^\circ$ Ag on Si(111) and a proposed $(\sqrt{3} \times \sqrt{3})R30^\circ$ Si structure on the *clean* surface provides strong support for MTL models. They have analyzed LEED I - V data for a $(\sqrt{3} \times 3)R30^\circ$ Si structure. The "vacancy model" they propose for this structure is precisely our domain 1 if the Ag atoms are replaced by a honeycomb of Si adatoms on the second Si layer. Furthermore, their LEED analysis finds the Si adatoms very close to the second Si layer, with $z = +0.28$, and a trimer contraction of $s = 0.65 \text{ \AA}$. Our values of $z = -0.1$ to -0.3 \AA and $s = 0.86 \text{ \AA}$ for Ag as adatom are thus very close to these, especially since Ag may bond more strongly and also has a larger effective radius. One can thus ask if the $(\sqrt{3} \times \sqrt{3})R30^\circ$ Si structure may also form in two domains. Finally, they have concluded from the similarity of the LEED I - V curves for both $(\sqrt{3} \times \sqrt{3})R30^\circ$ Ag and $(\sqrt{3} \times \sqrt{3})R30^\circ$ Si that the latter is responsible for the LEED pattern in both cases. Thus, they suggest that Ag is present in some sort of disordered array probably involving Ag penetration below

the surface and a diffuse interface. However, we disagree with this conclusion for several reasons: (i) Our polar-angle data rule out deeply buried Ag and thus also a diffuse interface. (ii) The structural similarity of our $(\sqrt{3} \times \sqrt{3})R30^\circ$ Ag model to that for $(\sqrt{3} \times \sqrt{3})R30^\circ$ Si suggests that the LEED I - V curves for the two should be nearly identical. (iii) Finally, the greater degree of fine structure seen in the LEED data for $(\sqrt{3} \times \sqrt{3})R30^\circ$ Ag could be due to the presence of large ordered domains of Ag MTL honeycombs consistent with the images seen in STM.⁴ We thus believe that Ag forms structures with long-range order, and that it would be interesting to reanalyze the $(\sqrt{3} \times \sqrt{3})R30^\circ$ Ag LEED data assuming either domain 1 or our proposed mixture of domains 1 and 2.

We thus conclude from this XPD study and other recent results that the most likely geometry for $(\sqrt{3} \times \sqrt{3})R30^\circ$ Ag on Si(111) involves a mixture of the two missing-top-layer honeycombs of Fig. 3(b). However, additional aspects such as the exact Ag coverage involved (our model requires $\frac{2}{3}$ ML), the metallic or semiconducting nature of this structure, and the expected differences in atomic positions and total energies for the two domains need further experimental and theoretical study.

We gratefully acknowledge the support of the Office of Naval Research under Contract No. N00014-87-K-0512 and of the National Science Foundation under Grant No. CHE83-20200.

*Present address: Laboratoire pour l'Utilisation du Rayonnement Electromagnétique, CNRS, 91405 Orsay, France.

†Present address: Optoelectronics Technology Research Laboratory, Tsukuba, Ibaraki 300-26, Japan.

¹Y. Terada, T. Yoshizuka, K. Oura, and T. Hanawa, *Surf. Sci.* **114**, 65 (1982).

²W. C. Fan, A. Ignatiev, H. Huang, and S. Y. Tong, *Phys. Rev. Lett.* **62**, 1516 (1989).

³(a) Y. Horio and A. Ichimiya, *Surf. Sci.* **133**, 393 (1983); (b) A. Ichimiya, S. Kohmoto, T. Fujii, and Y. Horio (unpublished).

⁴(a) E. J. van Loenen, J. E. Demuth, R. M. Tromp, and R. J. Hamers, *Phys. Rev. Lett.* **58**, 373 (1987); (b) R. J. Wilson and S. Chiang, *J. Vac. Sci. Technol. A* **6**, 800 (1988), and earlier references therein.

⁵(a) M. Aono, R. Souda, C. Oshima, and Y. Ishizawa, *Surf. Sci.* **168**, 713 (1986); (b) T. L. Porter, C. S. Chang, and I. S. T. Tsong, *Phys. Rev. Lett.* **60**, 1739 (1988); (c) R. S. Williams, R. S. Daley, J. H. Huang, and R. M. Charatan (unpublished).

⁶J. Stohr, R. Jaeger, G. Rossi, T. Kendelewicz, and I. Lindau, *Surf. Sci.* **134**, 831 (1983).

⁷(a) T. Takahashi, S. Wakatani, N. Okamoto, T. Ishikawa, and S. Kikuta, *Jpn. J. Appl. Phys.* **27**, L753 (1988); (b) E. Vlieg,

A. W. Denier v.d. Gon, J. F. v. d. Veen, J. E. Macdonald, and C. Norris, *Surf. Sci.* **209**, 100 (1989).

⁸M. Copel and R. Tromp, *Phys. Rev. B* **39**, 12688 (1989).

⁹S. Kono, K. Higashiyama, and T. Sagawa, *Surf. Sci.* **165**, 21 (1986).

¹⁰(a) S-H. Chou, A. J. Freeman, S. Grigoras, T. M. Gentle, B. Delley, and E. Wimmer, *J. Chem. Phys.* **89**, 5177 (1988); (b) C. T. Chan and K. M. Ho, *Surf. Sci.* **217**, 403 (1989); (unpublished).

¹¹(a) C. S. Fadley, *Prog. Surf. Sci.* **16**, 275 (1984); (b) R. A. Armstrong and W. F. Egelhoff, *Surf. Sci.* **154**, L225 (1985); (c) C. S. Fadley, *Phys. Scr.* **T17**, 39 (1987).

¹²(a) J. J. Rehr and R. C. Albers (unpublished); (b) D. J. Friedman and C. S. Fadley, *Electron Spectrosc.* (to be published).

¹³M. A. van Hove, S. Y. Tong, and M. H. Elconin, *Surf. Sci.* **64**, 85 (1977).

¹⁴M. Tochiwara and Y. Murata (private communication).

¹⁵M. Hanbuchen, M. Futamoto, and J. A. Venables, *Surf. Sci.* **147**, 433 (1984).

¹⁶E. L. Bullock, Ph.D. thesis, University of Hawaii, 1988 (unpublished).

¹⁷A. P. Kaduwela, G. S. Herman, D. J. Friedman, and C. S. Fadley (unpublished).